PROCEEDINGS, 43rd Workshop on Geothermal Reservoir Engineering
Stanford University, Stanford, California, February 12-14, 2018
SGP-TR-213

Fracture Network Characterization as input for Geothermal Energy Research: Preliminary data from Kuujjuaq, Northern Québec, Canada

M. M. Miranda, C. Dezayes, N. Giordano, I. Kanzari, J. Raymond and J. Carvalho

Institut national de la recherche scientifique. 490, rue de la Couronne, Québec (Québec) G1K 9A9 Canada

Centre d'études nordiques. 2405, rue de la Terrasse, Université Laval, Québec (Québec), G1V 0A6 Canada

Bureau de Recherches Géologiques et Minières. 3 avenue Claude-Guillemin BP 36009 45060 Orléans Cedex 2, France

Geosciences Center of University of Coimbra. Rua Silvio Lima, 3030-790 Coimbra, Portugal

mafalda_alexandra.miranda@ete.inrs.ca

Keywords: Fractures, Topology, Geothermal energy, Kuujjuaq, Canada

ABSTRACT

This research work is part of an ongoing project that aims to assess the potential of geothermal resources in Nunavik, northern Québec Canada, through shallow ground-source heat pumps (GSHP), underground thermal energy storage (UTES), deep enhanced/engineered geothermal systems (EGS) and deep borehole heat exchangers using the Inuit community of Kuujjuaq as case study. More specifically, this work represents a contribution for the evaluation of the exploitation of deep geothermal resources via EGS. The study of fractures' intrinsic properties and fracture networks are key aspects since the geothermal reservoir is developed through stimulation of the natural fracture system. Metric and topological properties of fractures were analyzed for that purpose.

The metric properties were acquired by the scanline sampling method. Observations were recorded from surface outcrops to identify the fracture intersection distance with the scanline, orientation, length, termination and aperture. Other parameters of interest, namely the number of sets, their spacing and density were estimated from these previous parameters. The measurements of fracture aperture were performed using a digital caliper. Equivalent fracture porosity was estimated as well. The topological properties of the system were evaluated by node counting. The proportion of the nodes was finally used to characterize the fracture network in terms of connectivity.

Field observation evidenced that the main orientations of the natural fractures populations are NNW-SSE and NNE-SSW. The orientation of the maximum principal stress $\sigma 1$ is assumed to be horizontal and oriented roughly NW-SE. The sector studied for topological properties is dominated by abutments (Y-nodes; 55 %), followed by fractures ending with isolated tips (I-nodes; 26 %), and cross-cutting fractures (X-nodes; 19.5 %). The ratio of number of branches to lines (3.33), the average number of connections per node (2.68), the average number of connections per line (3.69) and the average number of connections per branch (1.81) indicate that the system is partially connected, with a critical connectivity close to 4. It is also characterized by a high proportion of interconnected branches in doubly connected style. The potential hydraulic connectivity is estimated to be 0.46. This system is density-clustered and, besides the high proportion of Y-nodes, is not characterized by a high tortuosity.

The fractures show very high to low permeability and hydraulic conductivity; however, these values may be overestimated due to the measurements perform in rock surface exposed to weathering conditions that can alter the physical properties of the fractures. Nevertheless, their qualitative features can be combined with the expected fracture system connectivity to evaluate if the medium show valuable characteristics to be exploited for geothermal purposes.

This preliminary assessment of fracture system connectivity and potential fracture hydraulic properties suggest that hydraulic stimulation of natural fractures is feasible in the area surrounding the Inuit village of Kuujjuaq. If commercial reservoir temperature is available at reasonable depth, then this area has valuable conditions for the exploration of deep geothermal resources via EGS.

1. INTRODUCTION

This research work is part of an on-going project that aims to assess the potential of Nunavik geothermal resources through shallow ground-source heat pumps (GSHP), underground thermal energy storage (UTES), deep enhanced/engineered geothermal systems (EGS) and deep borehole heat exchangers for northern communities of Québec using the Inuit community of Kuujjuaq as case study. If geothermal technologies are proven viable in this village, then it can be possible to replicate the solution to other remote and off-grid communities to help reduce the fossil fuel consumption and greenhouse gases emissions.

A critical aspect to investigate, especially for EGS development, is the hydraulic connectivity provided by fracture networks. Fractures are present at all scales in the upper crust rocks, from microfractures with dimensions of microns to lineaments of several kilometers (Seeburger and Zoback, 1982). The geometry of the fracture system exerts a profound effect upon the hydro-mechanical properties of rocks (Seeburger and Zoback, 1982, Jing and Stephansson, 1997): fractures are the main pathways for water circulation, enabling the storage and movement of fluids or acting as barriers to water flow (Singhal and Gupta, 2010). The study of these discontinuities and the characterization of the fracture network are, thus, key inputs in geothermal systems modelling.

Fracture network modelling is of paramount importance for EGS, where the geothermal reservoir is developed by stimulation (hydraulic, thermal, or chemical) of the existing natural fractures to achieve sufficient permeability to produce adequate fluid flow rates of economic success (e.g., Genter et al., 2010; McClure and Horne, 2014). In low permeability rocks, the process of hydraulic stimulation is conceptualized as a complex network of newly forming fractures and/or natural fractures that slip and open (McClure, 2012 and references therein) according to the regional stress state. Hydraulic fractures propagate perpendicular to the minimum principal stress (Desroches and Bratton, 2000). Four conceptual models are commonly used for hydraulic stimulation: (1) pure open mode, (2) pure shear stimulation, (3) primary fracturing with shear stimulation leakoff and (4) mixed-mechanism stimulation (McClure, 2012; McClure and Horne, 2014). Thermal stimulation is carried out by injecting cold water into hot rocks to promote thermal contraction and in this way, create or enhance the fractures close to the borehole. Chemical stimulation removes clogging of pore spaces or enhance fracture permeability close to the borehole by means of acidic treatments (e.g., Schulte et al., 2010). Thus, the results presented in this work are going to be used in numerical models to simulate the behavior of a geothermal reservoir enhanced by hydraulic stimulation.

One key step to characterize the fracture networks is to estimate the number of fractures and their geometrical properties (Seifollahi et al., 2014), which are divided into metric properties and topological properties (Jing and Stephansson, 1997). The metric properties include several parameters (e.g., Singhal and Gupta, 2010), the most important being orientation, spacing, aperture and length. These features can vary under certain conditions, like a deformation process (Jing and Stephansson, 1997). The topological properties encompass the fractures' connectivity and do not change during continuous deformation processes (Jing and Stephansson, 1997).

Several methods are available to acquire the metric properties, including the scanline sampling, the window sampling and the circular scanline and window methods on exposed rock surfaces (Priest, 1993; Zeeb et al., 2013). The scanline sampling method (e.g., Priest, 1993) was used this work to collect the metrical features of the fractures on outcrops and the topological properties of the system was established by node counting (Sanderson and Nixon, 2015).

2. GEOLOGICAL AND STRUCTURAL CONTEXT

The study area is located in the Southeastern Churchill Province (Fig. 1). This part of the geological province has a tripartite structure caused by the oblique collisions of Nain-Core Zone-Superior cratons. The Torngat Orogen links the Nain and Core zone cratons, the New Québec Orogen connects the Core Zone and Superior cratons (e.g., Wardle et al., 2002). The dominant structural orientation is NNW-SSE characterized by numerous shear zones with several lengths and thrusting structures towards WSW (Simard et al., 2013 and references therein).

The west part of southeastern Churchill Province (SECP) is defined by three main deformation phases (D1 to D3) related to a continuous deformation process connected with New Québec orogeny. Phases D1 and D2 are associated to the compression generated during the collision between Core Zone and Superior and phase D3 is the result of the oblique component of that collision. D1 is responsible for the regional foliation, the NW-SE folds dipping to SW, and the existent thrusting faults. D2 produced the crenulation schistosity and E-W folds. D3 is associated to a late dextral strike-slip movement along the thrust faults and formed NW-SE folds dipping to SE (Simard et al., 2013 and references therein).

The study area within the SECP is in the Core Zone, and more specifically in the *Baie aux Feuilles* domain. The work was carried out in the *Complexe de Kaslac* (Areas 3 and 4; Fig. 1) and *Suite de la Baleine* (Areas 1 and 2; Fig. 1) lithological units located within this domain (Simard et al., 2013). The first consists of a complex mixture of intrusive gneiss to mylonitic rocks with composition varying from mafic to felsic. It is divided into four different units according to lithological and textural features: the diorite and quartz-diorite unit, the metagabbro garnet and magnetite-rich unit, the mafic to ultramafic intrusion unit, and the granitoid quartz-rich unit. The second lithological unit (*Suite de la Baleine*), within the surroundings of Kuujjuaq, is dominantly made of paragneiss. This unit is a set of quartz-feldspathic and pelitic to biotitic gneiss containing minor proportions of marble, calco-silicate rocks, amphibolite, quartzite, ultramafic schist, metaconglomerate and iron formations. The rocks present in the study area are Paleoproterozoic in age. The *Baie aux Feuilles* domain is characterized by an average orientation of the foliation plan of N338°E-30° and a regional foliation poles with orientation N127°E-16° (Simard et al., 2013).

Five zones were selected to carry out the fracture network modelling (Areas 1 to 5; Fig. 1). Areas 1 and 4 are located 2 km NE and NW of Kuujjuaq, respectively; area 2 is at 5 km in the SW direction; areas 3 and 5 are located approximately 1 km from the village, in the E and W directions, respectively. Area 1 is located close to the *Lac Pingiajjulik* fault and areas 3 and 4 in another regional fault intersecting the last one. *Lac Pingiajjulik* fault is a thrusting fault with dextral movement characterized by mylonitic texture and high recrystallization (Simard et al., 2013 and references therein). No regional fault has been mapped close to areas 2 and 5.

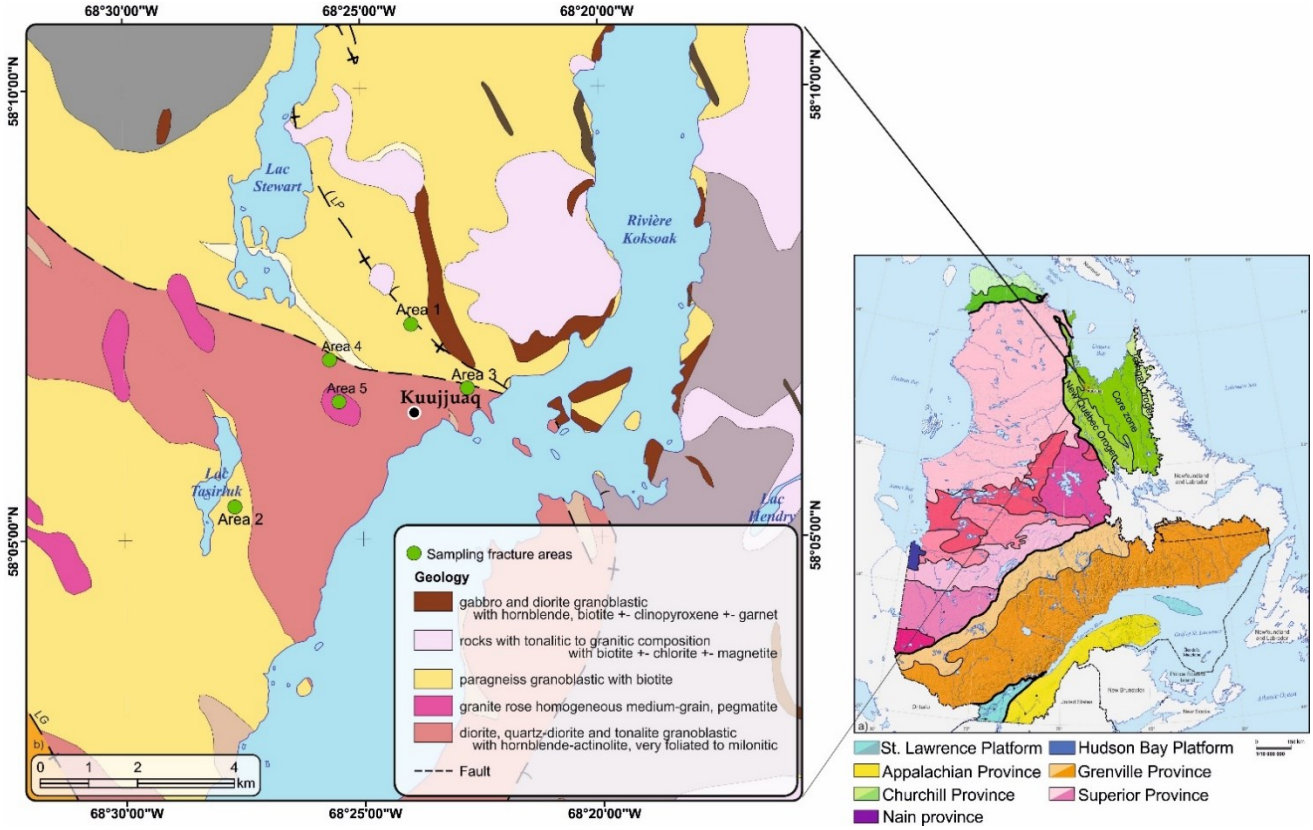

Figure 1: Right, geological setting of the geological provinces in northern Québec – Southeastern Churchill Province (adapted from Roy, 2012). Left, detailed geological map of the studied area with location of the five zones (areas 1 to 5) where the geometrical properties were acquired. *LP – Lac Pingiajjulik* fault, *LG – Lac Gabriel* fault.

3. METHODS AND TECHNIQUES

The scanline sampling method used in this work is based on data collection by direct observation of fracture characteristics intersecting a scanline on the rock mass surface providing one-dimensional information on fracture networks. Observations were carried out to determine: intersection distance with the scanline, orientation, length, termination and aperture. Others were estimated from the primary observations to calculate the number of sets, spacing and density. This method enables the characterization of metric properties in a quick way, but care must be taken to avoid orientation, truncation, censoring and size biases. In case of occurrence of these sampling biases, corrections need to be applied to avoid under- or over-estimations of the statistical parameters and to avoid prejudice of the fracture network characterization (Zhang and Einstein, 1998). The aperture measurements were performed using a caliper and the value measured is referred to as mechanical aperture. This aperture measured is a maximum value and is bias since the rock surface is exposed to weathering conditions that can lead to erosion of fracture walls. It was also possible to estimate the equivalent secondary (fracture) porosity (ϕ_f) based on the number of fractures per unit distance (s) and the mean mechanical aperture of the fractures (a_m) by the following equation (Singhal and Gupta, 2010)

$$\varphi_f = s \times a_m \tag{1}$$

The connectivity of the fracture network was evaluated based on Sanderson and Nixon (2015), considering that a two-dimensional fracture network consists of lines comprising one or more branches that, in turn, have a node at each end. The nodes can be isolated tips (I-nodes), crossing fractures (X-nodes) and abutments or splays (Y-nodes), as shown in Figure 2. The proportion of the nodes was then used to characterize the fracture network in terms of connectivity.

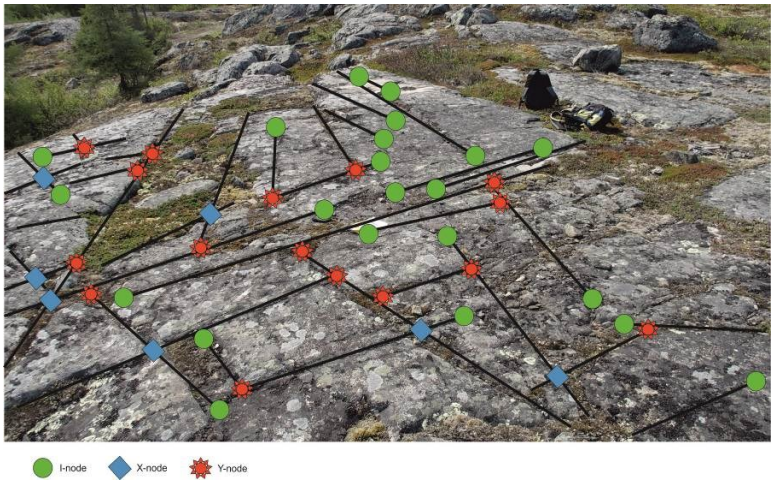

Figure 2: Example of node counting carried out during field work.

To count the number of lines (N_L) within a given area, the following relationship was used (Sanderson and Nixon, 2015):

$$N_L = \frac{1}{2}(N_I + N_Y) \tag{2}$$

Each branch is characterized by having two nodes and the number of branches (N_B) can be calculated as (Sanderson and Nixon, 2015):

$$N_B = \frac{1}{2}(N_I + 3N_Y + 4N_X) \tag{3}$$

The ratio of number of branches to lines is then (Sanderson and Nixon, 2015):

$$\frac{N_B}{N_L} = \frac{N_I + 3N_Y + 4N_X}{N_I + N_Y} \tag{4}$$

For each equation, N_I is the number of I-nodes, N_Y the number of Y-nodes and N_X stands for the number of X-nodes. Thus, it is possible to convert the number of lines to the equivalent number of branches and to understand the connections between each branch and classify the fracture system (Sanderson and Nixon, 2015). The average number of connections per node (C_N) can be calculated by (Saevik and Nixon, 2017):

$$C_N = \frac{N_I + 3N_Y + 4N_X}{N_I + N_Y + N_X} \tag{5}$$

The node counting also provide the average number of connections per line (C_L) and the average number of connections per branch (C_B). These values have been widely used as a measure of connectivity (Sanderson and Nixon, 2015 and references therein). C_L is given by:

$$C_L = 4\frac{N_Y + N_X}{N_I + N_Y} \tag{6}$$

and C_B by:

$$C_B = \frac{3N_Y + 4N_X}{N_B} \tag{7}$$

Beyond the connectivity, the termination index was also evaluated. This provides information about the interconnections between the fractures and allows to classify the persistence of the several fractures present (Priest, 1993; Sousa, 2007). The termination index (T_i) is calculated with the procedure of ISRM on (1978), based on the number of discontinuity traces that terminate in intact rock (N_I), the number of discontinuities that terminate at another discontinuity (N_A) and number of discontinuities in which termination is obscured (N_O):

$$T_{\mathrm{i}}(\%) = \frac{100 N_{\mathrm{I}}}{N_{\mathrm{I}} + N_{\mathrm{A}} + N_{\mathrm{O}}} \tag{8}$$

To calculate the potential fracture transmissivity and permeability and fractured rock mass hydraulic conductivity, the mechanical aperture (a_{m}) measured by scanline sampling can be transformed to hydraulic aperture a_{h} (mm) with the following equation proposed by Lee et al., (1996):

$$a_{\mathrm{h}} = \frac{a_{\mathrm{m}}^2}{JRC^{2.5}} \tag{9}$$

where *JRC* is joint roughness coefficient that was assumed equal to 3 for the study area, which is the minimum for natural fractures to account for more realistic conditions (Singhal et al., 2010 and references therein).

The potential fracture transmissivity T_{f} ($\mathrm{m^2\ s^{-1}}$) of the studied zones can be calculated using the cubic law by (e.g., Chesnaux et al., 2009):

$$T_{\mathrm{f}} = \frac{a_{\mathrm{h}}^3}{12} \frac{\rho g}{\mu} \tag{10}$$

where a_{h} (m) stands for the hydraulic aperture of the fractures, ρ ($\mathrm{kg\ m^{-3}}$) is the fluid density, g ($\mathrm{m\ s^{-2}}$) is the gravitational acceleration and μ ($\mathrm{kg\ m^{-1}\ s^{-1}}$) is the dynamic fluid viscosity.

The potential fracture permeability k_{f} ($\mathrm{m^2}$) can be defined as (e.g., Chesnaux et al., 2009; Singhal and Gupta, 2010):

$$k_{\mathrm{f}} = \frac{a_{\mathrm{h}}^3}{12} \tag{11}$$

The fractured rock mass potential hydraulic conductivity K_{f} ($\mathrm{m\ s^{-1}}$) can be calculated by (Singhal and Gupta, 2010):

$$K_{\mathrm{f}} = \frac{g a_{\mathrm{h}}^3}{12 \nu s} \tag{12}$$

where s (m) is fracture spacing (Fig. 4c) and υ ($\mathrm{m^2\ s^{-1}}$) is the coefficient of kinematic viscosity.

4. RESULTS

4.1 Metric properties

The following division in classes was assumed for the statistical analysis of the metric properties of fractures based on alteration and length: master joints, if no alteration is visible and fractures have lengths > 2 m; secondary joints, if no alteration is visible and fractures have lengths < 2 m; altered joints, if alteration is visible; and faults, if the fractures exhibit shearing displacement (mode II – sliding mode of fractures). This division is important as each one of these classes is characterized by intrinsic properties that behave differently when subject to hydraulic stimulation.

Mechanical aperture was classified according to ISRM (1978) as follows: very tight, if aperture < 0.1 mm; tight, if aperture is between 0.1 – 0.25 mm; partly open, if aperture is between 0.25 – 0.50 mm; open, if aperture is between 0.50 – 2.50 mm; moderately wide, if aperture is between 2.50 – 10.0 mm; wide, if aperture > 10.0 mm.

Area 1 is located in paragneiss. Fractures have two equally preferential orientations; NNW-SSE and ENE-WSW (Fig. 3). The master joints have a length varying from 2.4 to 25 m minimum (Fig. 4). A possible shear zone was observed to have orientation NW-SE, showing a wide aperture of 49 mm. The master joints show mechanical apertures from close to wide and the secondary joints from close to moderately wide (Fig. 4). The average spacing between fractures is 1.1 m, with a standard deviation of 0.7 (Table 1). The fracture density of this area is 1.03 $\mathrm{m^{-1}}$. Both master and secondary joints are systematic. The fracture sets observed are conjugate and orthogonal, based on the dihedral angle measured from the intersection of sets. In terms of relative timing of joint formation, the ENE-WSW sets are possibly older than the NNW-SSE, since the first show signs of movement in the intersection with the last set. The equivalent secondary (fracture) porosity in this area calculated by Eq. (1) is on average 7 %.

As area 1, area 2 is located in paragneiss and has preferential fracture orientation E-W with scattered fractures along NNE-SSW (Fig. 3). The master joints have a length varying from 2 to 10 m and mechanical apertures from close to wide (Fig. 4). The secondary joints have a length in the range of 0.4 to 1 m and mechanical apertures that vary from close to wide (Fig. 4). The average spacing between fractures in this area is 1.1 m, with a standard deviation of 1.2 (Table 1). A fracture density of 1.23 $\mathrm{m^{-1}}$ was estimated for this area. Both master and secondary joints are systematic. The fracture sets observed are conjugate, based on the dihedral angle measured from the intersection of sets. The equivalent secondary (fracture) porosity in this area is 6 %.

Area 3 is located in diorite, close to the contact (or faulted contact) with paragneiss. Fractures are oriented preferentially to NW-SE, with scattered fractures oriented to NE-SW (Fig. 3). The master joints have a length varying from 2 to 11 m, the secondary joints have a length in the range of 0.2 to 1.5 m, and the altered joints have a length of 0.3 to 5.2 m (Fig. 4). The altered joints have schist filling the apertures. All classes have closed apertures (Fig. 4), which consequently gives an average equivalent secondary (fracture) porosity of 0.1%.

Area 4 is also located in diorite, close to the contact (or faulted contact) with paragneiss. This area shows the same fracture orientations as in area 3, which is a preferential orientation to NW-SE and scattered fractures oriented to NE-SW (Fig. 3). Most fractures observed were systematic master joints with mechanical apertures varying from close to wide (Fig. 4). The average spacing between fractures and standard deviation is 0.8 m and 0.6, respectively (Table 1). Regarding fracture density, a value of 1.35 m^{-1} was calculated. The fracture sets observed are conjugate and orthogonal, based on the dihedral angle measured from the intersection of sets. In terms of relative timing of joint formation, the NW-SE set is possibly older than the NE-SW, since the first shows signs of movement in the intersection with the last set. The equivalent secondary (fracture) porosity in this area is on average 0.4 %.

Area 5 is located in a granite, where the preferential orientation of the fractures is NNW-SSE (Fig. 3). Most fractures observed were systematic master joints with mechanical apertures varying from close to moderately wide (Fig. 4). The average spacing between fractures is 0.6 m, with a standard deviation of 0.4 (Table 1). The fracture density is 1.88 m^{-1}. The fracture sets observed are conjugate and orthogonal, based on the dihedral angle measured from the intersection of sets. The equivalent secondary (fracture) porosity in this area is on average 0.2 %.

The *Lac Pingiajjulik* fault is an important regional structure present within the study area. This structure is a transpressional fault and its main orientation is NW-SE (Fig. 3). It can be noted from the same figure that the most prominent system of surface fractures observed in the studied zones are oriented NNW-SSE and NNE-SSW. A thrust fault regime implies minimum principal stress ($\sigma 3$) as the vertical stress (S_v) and the maximum ($\sigma 1$) and intermediate ($\sigma 2$) principal stresses as maximum (S_H) and minimum (S_h) horizontal stresses, respectively. Due to the deformation phase D3, $\sigma 3$ is probably deviated from vertical and correspond to S_h. As the orientation of *Lac Pingiajjulik* fault and the remaining regional structures is roughly NW-SE, this means that $\sigma 1$ had a NE-SW compressional direction.

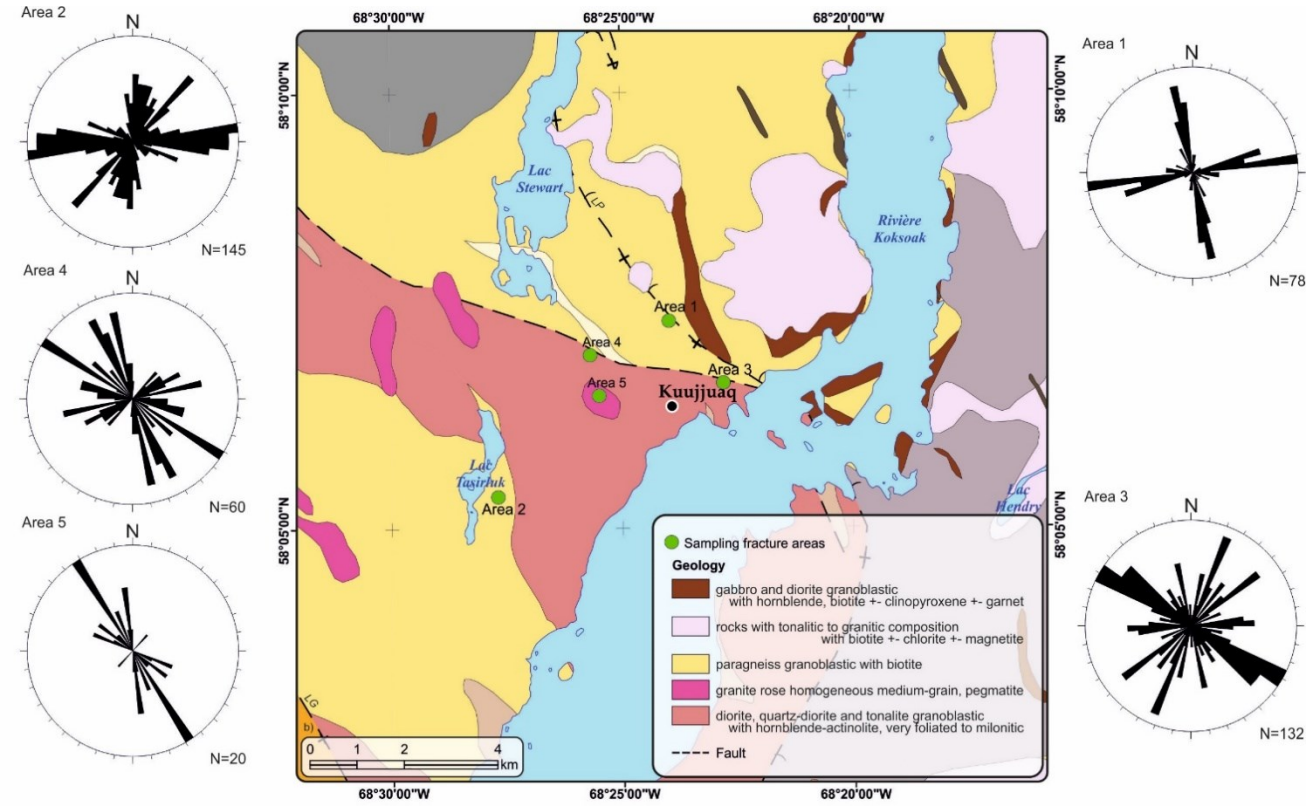

Figure 3: Rose diagrams for each examined zone associated with their position in the geological map.

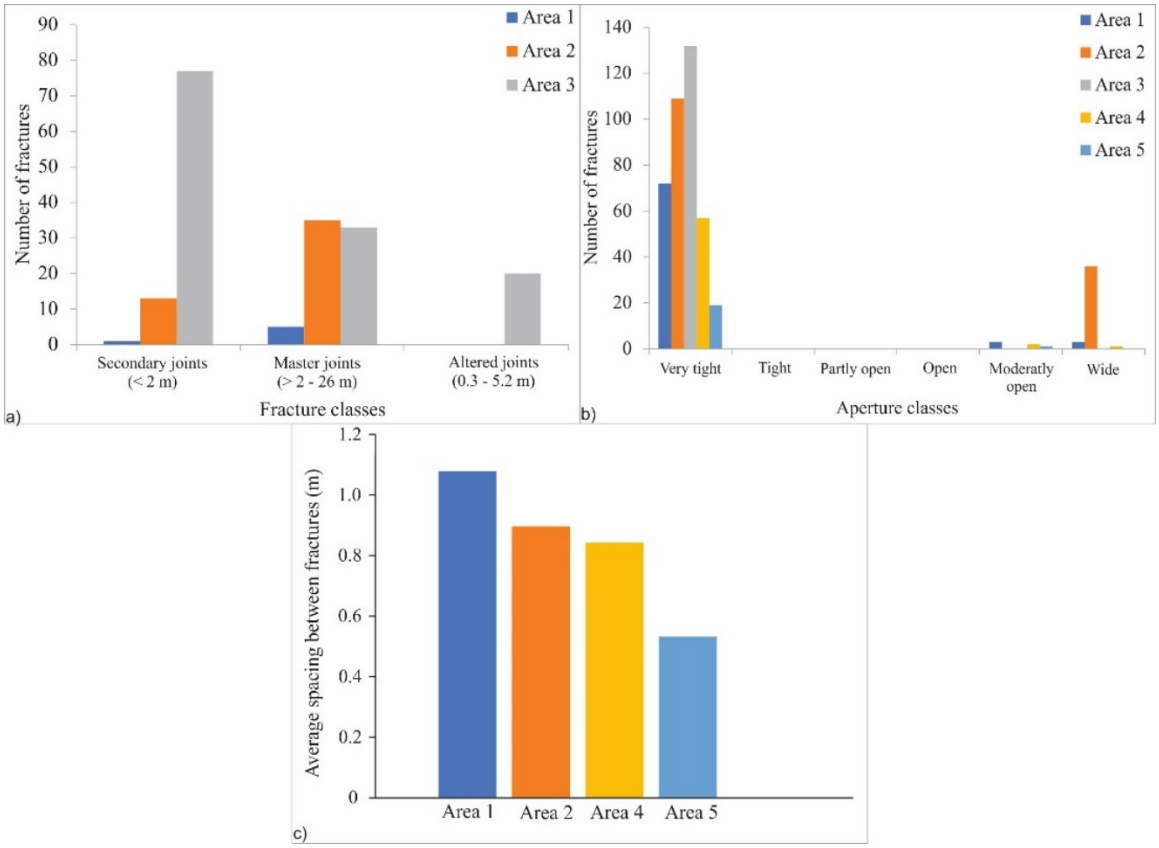

Figure 4: Histograms of a) fracture length, b) mechanical aperture and c) average fracture spacing for each area studied.

Table 1: Summary of the results obtained from scanline sampling.

	Area 1			Area 2			Area 3	Area 4			Area 5		
Orientation	NNW-SSE and ENE-WSW			E-W with scattered fractures NNE-SSW			NW-SE with scattered fractures NE-SW	NW-SE with scattered fractures NE-SW			NNW-SSE		
Length (m)	2 – 25(min)			0.2 – 10			0.2 – 11						
Aperture (mm)	0 – 49.09			0 – 48.85			> 0.1	2.32 – 11.94			4.92		
Spacing (m)	μ	σ	CV	μ	σ	CV		μ	σ	CV	μ	σ	CV
	1.1	0.7	0.6	1.1	1.2	1.1		0.8	0.6	0.7	0.6	0.4	0.7

μ - arithmetic average; σ – standard deviation; CV – coefficient of variation.

4.2 Topological properties

The topological properties analysis was carried out in a sector within area 2, where the node (Fig. 5a) and termination (Fig. 5b) counting was performed. The total number of nodes counted is 128, of which 33 are isolated tips (I-nodes), 25 are crossing fractures (X-nodes), and 70 are abutments (Y-nodes). Regarding the terminations, 13 were considered discontinuities that terminates in intact rock material (I-type), 50 terminate in another discontinuity (A-type) and 17 have an obscured termination (O-type). These two parameters indicate that this sector is characterized by a system dominated by abutting fractures terminations, since 55 % are Y-nodes and 62.5 % are A-type terminations. The isolated fractures correspond to 26 % of the system and the cross-cutting fractures 19.5 %. Moreover, 21 % of the fractures observed show obscured terminations (O-type) and 16 % terminates in intact rock (I-type).

Applying Eqs. 2 to 7 to the node counting, there is 51.5 lines observed in the sector studied (Eq. 2) and 171.5 branches (Eq. 3). The ratio of number of branches to lines is 3.33 (Eq. 4), while the number of connection per node is 2.68 (Eq. 5). The number of connections per line for the studied sector is 3.69 (Eq. 6) and the number of connections per branch is 1.81 (Eq. 7). The termination index gives a value of 16 % (Eq. 8).

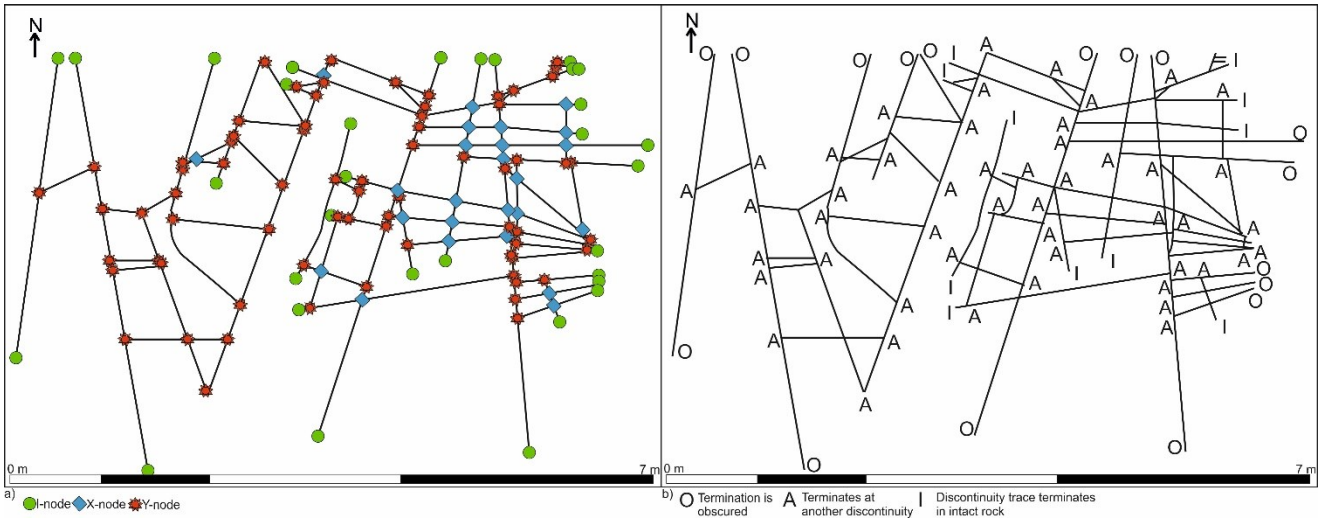

Figure 5: a) node counting and b) termination counting in a sector of area 2

4.3 Potential fracture transmissivity and permeability and fractured rock mass potential hydraulic conductivity

The hydraulic apertures calculated by Eq. (9) are higher than expected in non-weathered fractures as the mechanical apertures were measured in surface rock exposed to weathering conditions, which leads to high values of transmissivity, permeability and hydraulic conductivity.

To calculate the potential average fracture transmissivity (Eq. 10), pure water was assumed with ρ as 10^3 kg m^{-3}, g as 9.81 m s^{-2} and μ as 10^{-3} kg m^{-1} s^{-1}. For area 1 to 5, the potential average fracture transmissivity is 6.7, 5.6, 2.2 ×10^{-13}, 7.9 ×10^{-6} and 3.9 ×10^{-7} m^2 s^{-1}, respectively (Table 2). The potential average fracture permeability (Eq. 11) for area 1 to 5 is 2.7 x10^{-5}, 2.4 ×10^{-5}, 3.4 ×10^{-14}, 3.8 ×10^{-9} and 5.1 ×10^{-10} m^2, respectively (Table 2). To calculate the fractured rock mass potential hydraulic conductivity (Eq. 12), υ was assumed equal to 1.0 x 10^{-6} m^2 s^{-1}. The hydraulic conductivity of area 1 to 5 is 6.2, 6.2, 2.7 × 10^{-13}, 9.3 × 10^{-6} and 2.0 × 10^{-6} m s^{-1}, respectively (Table 2).

Table 2: Equivalent fracture porosity (φ_f), potential fracture transmissivity (T_f), potential fracture permeability (k_f) and fractured rock mass potential hydraulic conductivity (K_f).

	Area 1	Area 2	Area 3	Area 4	Area 5
ϕ_f (%)	7	6	0.1	0.4	0.2
T_f (m^2 s^{-1})	6.7	5.6	2.2 x10^{-13}	7.9 x10^{-6}	3.9 x10^{-7}
k_f (m^2)	2.7 x10^{-5}	2.4 x10^{-5}	3.4 x10^{-14}	3.8 x10^{-9}	5.1 x10^{-10}
K_f (m s^{-1})	6.2	6.2	2.7 x10^{-13}	9.4 x10^{-6}	2.0 x10^{-6}

5. DISCUSSION

5.1 Fracture network connectivity

In a random continuum percolation model, the fracture system is uniformly clustered with all fractures connected by fracture intersections (X-nodes) and ending as isolated line tips (I-nodes). Y-nodes do not form in these kinds of systems (Manzocchi, 2002 and references therein). On the other hand, in natural fracture systems, the connectivity is achieved through a combination of fracture intersections (X-nodes) and abutments (Y-nodes). Y-nodes are important contributors to the connectivity of natural systems and a system with high proportion of fractures ending as abutments is characterized by fewer I-nodes. The critical density is low in natural fracture systems and the percolation cluster resembles closely to the percolation backbone (Manzocchi, 2002 and references therein). Node counting indicated that the fracture system studied is composed by 55 % of Y-nodes, 26 % of I-nodes and 19.5 % of X-nodes. Generally, natural fracture systems have Y:X node ratios higher than 1 (Manzocchi, 2002), correlating to the system studied that has a ratio of 2.8.

The number of nodes counted can be plotted in a ternary diagram (Fig 6). The position on the diagram not only characterizes the nature of the connectivity but also quantifies this connectivity (Barton and Hsieh, 1989).

The ratio of number of branches to lines enables to characterize the type of fracture system (Eq. 4). A fracture system composed by isolated tips has N_B/N_L close to 1 and is disconnected; in turn, a fracture system composed by long, closely-spaced, cross-cutting fractures is dominated by X-nodes and the ratio of number of branches to lines would tend to infinity, meaning a highly connected fracture system. A fracture system with dominating Y-nodes will have a N_B/N_L of 3 (Sanderson and Nixon, 2015). The N_B/N_L in the studied system amounts to 3.33 (Fig. 6a), meaning a partially connected fracture network.

The average number of connections per node varies from 1 to 4 (C_N; Eq. 5), in which the maximal value is only attained when all the nodes are X-nodes (Saevik and Nixon, 2017). C_N is 2.68 for the sector studied, highlighting the prevalence of Y-nodes, followed by I- and X-type terminations.

A fracture system becomes connected when the critical connectivity value is higher than 2, while a lower value means an unconnected system and no percolation threshold exist (Manzocchi, 2002). Moreover, if a system has a critical connectivity between 2 and 3.11, it means that it contains fracture orientation populations clustered independently. A uniformly clustered system is characterized by a critical connectivity of 3.11. The critical connectivity for density-clustered systems is higher than 3.11 and the more intense is the clustering the higher this value. Using the number of connections per line to calculate the critical connectivity (C_L; Eq. 6), the system studied as a value of 3.69 (Fig. 6b), meaning that it is connected and may be a density-clustered system.

The number of connections per branch can be used to calculate the connectivity of a system (C_B; Eq. 7) and it gives a value in the range 0 to 2 (Sanderson and Nixon, 2015), in which the maximal value is attained when no fracture terminates as isolated tips. This will be the optimal fracture system, with no dead-ends and isolated branches, with a hydraulic connectivity close to the maximal (Saevik and Nixon, 2017). C_B is 1.81 for the studied sector, indicating that this fracture system has a small amount of dead-ends and may have a good hydraulic connectivity (Fig. 6c).

Each branch, composed by two end-nodes, can be classified as I-I, I-X, I-Y, Y-Y, Y-X, and X-X, or simply as isolated branches (I-I), partly connected branches (I-C), and doubly connected branches (C-C). Partly connected means branches with I-X and I-Y node ends, while doubly connected are branches that end with Y-Y or Y-X nodes (Sanderson and Nixon, 2015 and references therein). The value of C_B observed in the studied sector indicate a high proportion of interconnected branches in doubly connected style (Fig. 6d).

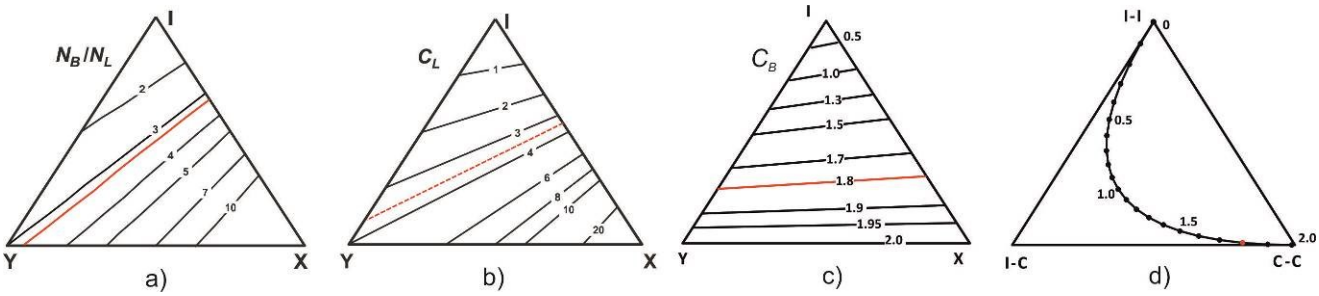

Figure 6: Triangular plots of node proportion with network topology showing a) the ratio of number of branches to lines (N_B/N_L = 3.3), b) the number of connections per line (C_L = 3.7), c) the number of connections per branch (C_B = 1.8) and d) the branch classification plot based on C_B values. Observed values described in this study are highlighted in red (adapted from Sanderson and Nixon, 2015).

The termination index does not provide complete information about the system connectivity (T_i; Eq. 8) but permits to classify the persistence of the joints and understand the susceptibility for rock failure. A large value of the termination index, identified by a large proportion of joints with termination on intact rock, means a rock mass stiffer and stronger than one with a lower index (e.g., Priest, 1993; Sousa, 2007). The sector studied has a T_i of 16 %, showing a rather weak rock mass due to the prevalence of discontinuities that terminate in another discontinuity (A-type; 62.5 %).

The high prevalence of fractures that terminate against each other suggest that this system have a high tortuosity, as Y-nodes usually force the fluid to follow a tortuous path through the network, and a lower hydraulic connectivity (Saevik and Nixon, 2017). The potential hydraulic connectivity (f) of the system studied can be calculated following the approach described in Saevik and Nixon (2017):

$$f = 2.94 \times C_f - 2.13 \tag{13}$$

in which C_f is the average number of connections per fracture, which is calculated by (Saevik and Nixon, 2017):

$$C_f = \frac{4N_X + 2N_Y}{4N_X + 2N_Y + N_I} \tag{14}$$

The hydraulic connectivity varies within the range 0.0 to 0.8 and the obtained value for the system studied is 0.46 (Fig. 7). Besides the high percentage of Y-nodes, the system is not characterized by a high tortuosity.

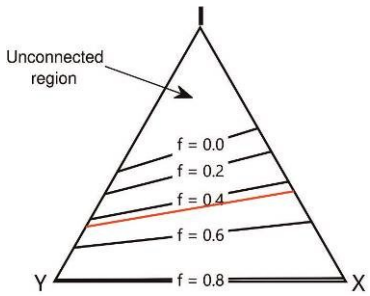

Figure 7: Triangular plot for hydraulic connectivity (*f*). The red line represents the hydraulic connectivity calculated for the fracture network system analyzed (adapted from Saevik and Nixon, 2017).

5.2 Fracture clustering

The coefficient of variation (CV) of fracture separations was used to estimate the fracture clustering. This coefficient is based on the standard deviation of fracture separations divided by the mean separation value. Fractures uniformly clustered with a purely exponential distribution have CV equals to 1. In the case of fractures distribution in a regular pattern, CV is less than 1 and fractures are anticlustered. If CV is higher than 1, it means that fractures have a heterogeneous distribution and they are clustered (e.g., Gillespie et al., 1999; Manzocchi, 2002). A $0 < CV < 1$ can also be related with the randomly oriented and positioned scanline that records fractures from different populations (Manzocchi, 2002) and a fracture system composed by systematic joints in which joint spacing is controlled by bed thickness (Gillespie et al., 1999). Clustered fracture systems with $CV > 1$ can be density-clustered, for scanlines recording fractures of different populations, or orientation-clustered, for scanlines recording fractures of only one population (Manzocchi, 2002). Spacing between fractures measured from scanline sampling indicates that area 1 is characterized by a CV of 0.62 (Table 1), while area 2 by CV of 1.1. The CV calculated for areas 4 and 5 is 0.7.

Areas 1, 4 and 5 have factures with a CV less than 1, meaning that these systems are characterized by anticlustered fractures and the systems have a regular pattern of fractures distribution. The CV values obtained additionally show that the fractures were recorded through a randomly oriented and positioned sample line and orientations from different populations were documented. Area 2, in turn, has fractures with a CV higher than 1, meaning that the fractures are clustered and distributed in a heterogeneous pattern. This area is characterized as a density-clustered system due to the value of critical connectivity of 3.69 (C_L; Fig. 7b).

5.3 Potential fracture transmissivity and permeability and fractured rock mass potential hydraulic conductivity

Areas 1 and 2 are characterized by very high fracture permeability and hydraulic conductivity; area 3 by moderate to low fracture permeability and low fracture hydraulic conductivity; and areas 4 and 5 by high fracture permeability and low fracture hydraulic conductivity (Table 2). Permeability and hydraulic conductivity of fractures have a direct proportionality relation, which is seen in most areas except the two-last studied. Referenced values for crystalline rocks in terms of rock mass porosity is 0 to 5 % for dense crystalline rocks, 5 to 10 % for fractured crystalline rocks and 20 to 40 % for weathered crystalline rocks (Singhal and Gupta, 2010 and references therein). The expected range of rock mass permeability and hydraulic conductivity are 1 to 10^{-4} D and 10^{-5} to 10^{-9} m s^{-1} for fractured and weathered crystalline rocks, respectively, and 10^{-3} – 10^{-8} D and 10^{-8} – 10^{-13} m s^{-1} for massive rocks, respectively (Singhal and Gupta, 2010). The porosities calculated from Eq. 1 for the 5 areas studied and mentioned in subsection 4.1 fall into the fractured crystalline rock mass field for areas 1 and 2, with porosities of 7 % and 6 % respectively, and the remaining areas into the dense crystalline rocks field.

6. CONCLUSIONS

This paper describes the preliminary results of the fracture network analysis in Kuujjuaq. The main orientations of the natural fractures populations of the studies areas are NNW-SSE and NNE-SSW. The orientation of the maximum principal stress $\sigma 1$ is assumed to be horizontal and the minimum principal stress $\sigma 3$ is still unknown, which can be vertical or horizontal and most likely slightly deviated from vertical. The maximum principal stress $\sigma 1$ was oriented NE-SW during *Lac Pingiajjulik* fault formation, as this regional fault was formed by compression and it is oriented roughly NW-SE.

The sector studied for topological properties is dominated by abutments (Y-nodes; 55 %), followed by fractures ending with isolated tips (I-nodes; 26 %) and cross-cutting fractures (X-nodes; 19.5 %). The Y:X node ratio is 2.8. The ratio of number of branches to lines (N_B/N_L=3.33), the average number of connections per node (C_N=2.68), the average number of connections per line (C_L=3.69) and the average number of connections per branch (C_B=1.81) all indicates that the system studied is partially connected, with a critical connectivity close to 4. It is also characterized by a high proportion of interconnected branches in doubly connected style. The termination index is 16%. The potential hydraulic connectivity (*f*) is estimated to be 0.46. This system is density-clustered and besides the high proportion of Y-nodes, it is not characterized by a high tortuosity. The data described in this article will be used in discrete fracture network models to evaluate the fluid flow within the medium and to assess the viability of a geothermal reservoir created by hydraulic stimulation.

The equivalent porous media showed very high to low permeability and hydraulic conductivity. These values are dependent on the fracture hydraulic aperture and spacing. Uncertainty is associated with the numerical values obtained since the apertures measured correspond to rock surface exposed to weathering effects that can alter the properties of the fractures. Nevertheless, their qualitative features can be

combined with the expected fracture system connectivity to evaluate if the medium show valuable characteristics to be exploited for geothermal purposes.

The orientation of the minimum principal stress is still unknown and further studies are needed to better define this parameter playing a major role in the development of hydraulic fractures. Studies regarding the magnitude of the principal stresses will be performed and the mechanical properties of the rocks (Young's modulus, bulk modulus, shear modulus, and Poisson's ratio) will be analyzed, due to their influence on how the system would behave during stimulation. The rock matrix porosity and permeability will be obtained by a combined gas permeameter and porosimeter device to evaluate the bulk hydraulic properties of the medium (Raymond et al., 2017).

The area surrounding the Inuit village of Kuujjuaq appears to have favorable conditions for the exploitation of deep geothermal resources via EGS if the minimum principal stress is oriented in such a way that hydraulic stimulation of natural fractures could be carried out in order to increase the connection of the fracture system. Shallow geothermal applications such as UTES would be feasible in locations where the rock mass hydraulic conductivity is moderate to low, in order to prevent heat losses from the underground storage volume. On the other hand, GSHP systems would benefit of highly permeable media. Numerical simulations are ongoing to evaluate the amount of energy that can be extracted or stored and to define the long-term efficiency and sustainability of these geothermal heat production modes.

NOMENCLATURE

a_h	Hydraulic aperture (m)
a_m	Mechanical aperture (mm)
C_B	Number of connections per branch
C_f	Number of connections per fracture
C_L	Number of connections per line
C_N	Number of connections per node
f	Hydraulic connectivity
g	Gravitational acceleration (m s^{-2})
JRC	Joint roughness coefficient
K_f	Fractured rock mass potential hydraulic conductivity (m s^{-1})
k_f	Potential fracture permeability (m^2)
N_A	Number of discontinuities that terminate at another discontinuity
N_B/N_L	Number of branches to lines
N_I	Number of discontinuity traces that terminate in intact rock
N_I	Number of I-nodes
N_L	Number of lines
N_O	Number of discontinuities in which termination is obscured
N_Y	Number of Y-nodes
N_X	Number of X-nodes
s	Fracture spacing (m)
T_f	Potential fracture transmissivity (m^2 s^{-1})
T_i	Termination index (%)
μ	Dynamic fluid viscosity (kg m^{-1} s^{-1})
ν	Coefficient of kinematic viscosity (m^2 s^{-1})
ρ	Fluid density (kg m^{-3})
ϕ_f	Secondary (fracture) porosity (%)

ACKNOWLEDGEMENTS

The authors would like to thank the Institut nordique do Québec (INQ) that financial the research activities through the *Chaire de recherche sur le potentiel géothermique du Nord* awarded to Jasmin Raymond and the Labex DRIIHM for supporting the activity of Chrystel Dezayes.

REFERENCES

Barton, C.C., and Hsieh, P.A.: Physical and hydrological-flow properties of fractures, *Field Trip Guidebook*, 28th International Geological Congress: Environmental, Engineering and Urban Geology in the United States 2, AGU, Washington D.C., US (1989).

Chesnaux, R., Allen, D.M., and Jenni, S.: Regional fracture network permeability using outcrop scale measurements, *Enginnering Geology*, **108**, (2009), 256-271.

Dershowitz, W.S., and Einstein, H.H.: Characterizing rock joint geometry with joint system models, *Rock Mechanics and Rock Engineering*, **21**, (1988), 21-51.

Desroches, J., and Dowell, S.: Formation Characterization: Well Logs, in M.J. Economides and K.G. Nolte (Eds), *Reservoir Stimulation*, Wiley, (2000), 114-139.

Genter, A., Evans, K., Cuenot, N., Fritsch, D., and Sanjuan, B.: Contribution of the exploration of deep crystalline fractured reservoir of Soultz to the knowledge of enhanced geothermal systems (EGS), *Comptes Rendus Geoscience*, **342**, (2010), 502-516.

Gillespie, P.A., Johnston, J.D., Loriga, M.A., McCaffrey, K.J.W., Walsh, J.J., Watterson, J.: Influence of layering on vein systematics in line samples, in K.J.W. McCaffrey, L. Lonergan and J.J. Wilkinson (Eds), *Fractures, Fluid Flow and Mineralization*, Geological Society, London, Special Publications, **155**, (1999), 35-56.

ISRM: International Society for Rock Mechanics Commission on Standardization of Laboratory and Field Tests suggested methods for the quantitative description of discontinuities in rock masses, *International Journal of Rock Mechanics and Mining Sciences & Geomechanics Abstracts*, **15**, 319-368.

Jing, L., and Stephansson, O.: Network topology and homogenization of fractured rocks, in B. Jamtveit and B.W. Yardley (Eds), *Fluid Flow and Transport in Rocks – Mechanisms and effects*, Chapman & Hall, (1997), 191-202.

Lee, C.F., Zhang, J.M., and Zhang, Y.X.: Evaluation and origin of the ground fissures in Xian, China, *Engineering Geology*, **43(1)**, (1996), 45-55.

Manzocchi, T.: The connectivity of two-dimensional networks of spatially correlated fractures, *Water Resources Research,* **38(9)**, 1162-1182.

McClure, M.: *Modeling and characterization of hydraulic stimulation and induced seismicity in geothermal and shale gas reservoirs*, Stanford University, (2012), 369 pp.

McClure, M.W., and Horne, R.N.: An investigation of stimulation mechanisms in Enhanced Geothermal Systems, *International Journal of Rock Mechanics & Mining Sciences*, **72**, (2014), 242-260.

Priest, S.D.: *Discontinuity Analysis for Rock Engineering*, Chapman & Hall, (1993), 489 pp.

Raymond, J., Comeau, F.A., Malo, M., Blessent, D., and López Sánchez, I.J.: The Geothermal Open Laboratory: a free space to measure thermal and hydraulic properties of geological materials, UNESCO IGCP636 Annual Meeting, Santiago de Chile, (2017).

Roy, C.: *The great geological domains of Québec*, Ressources naturelles Québec, (2012).

Saevik, P.N., and Nixon, C.W.: Inclusion of Topological Measurements into Analytic Estimates of Effective Permeability in Fractured Media, *Water Resources Research*, **53**, (2017), 9424-9443.

Sanderson, D.J., and Nixon, C.W.: The use of topology in fracture network characterization, *Journal of Structural Geology*, **72**, (2015), 55-66.

Schuelte, T., Zimmermann, G., Vuataz, F., Portier, S., Tischner, T., Junker, R., Jatho, R., and Huenges, E.: Enhancing Geothermal Reservoirs, in E. Huenges (Ed), *Geothermal Energy Systems*, Wiley, (2010), 173-243.

Seeburger, D.A., and Zoback, M.D.: The Distribution of Natural Fractures and Joints at Depth in Crystalline Rock, *Journal of Geophysical Research*, **87(B7)**, (1982), 5517-5534.

Seifollahi, S., Dowd, P.A., and Xu, C.: An enhanced stochastic optimization in fracture network modelling conditional on seismic events, *Computers and Geotechnics*, **61**, (2014), 85-95.

Simard, M., Lafrance, I., Hammouche, H., and Legouix, C.: *Géologie de la région de Kuujjuaq et de la baie d'Ungava*, Gouvernement du Québec, (2013), 62 pp.

Singhal, B.B.S., and Gupta, R.P.: *Applied Hydrogeology of Fractured Rocks*, Springer, (2010), 429 pp.

Sousa, L.M.O.: Granite fracture index to check suitability of granite outcrops for quarrying, *Engineering Geology*, **92(3-4)**, (2007), 146-159.

Wardle, R.J., James, D.T., Scott, D.J., and Hall, J.: The southeastern Churchill Province: synthesis of a Paleoproterozoic transpressional orogen, *Canadian Journal of Earth Sciences*, **39**, (2002), 639-663.

Zhang, L., and Einstein, H.H.: Estimating the Mean Trace Length of Rock Discontinuities, *Rock Mechanics and Rock Engineering*, **31(4)**, 217-235.

Zeeb, C., Gomez-Rivas, E., Bons, P.D., and Blum, P.: Evaluation of sampling methods for fracture network characterization using outcrops, *AAPG Bulletin*, **97(9)**, (2013), 1545-1566.